Seakeeping Characteristics of the Amphibious Assault Landing Craft

Allen H. Magnuson* and Richard F. Messalle†
David W. Taylor Naval Ship Research and Development Center, Bethesda, Md.

The predicted response characteristics of the JEFF Amphibious Assault Landing Craft while running on cushion in waves are presented. The vertical plane motion responses were calculated using model towing tank data obtained from oscillator tests and captive model wave excitation tests. Results are presented in terms of frequency response functions, response amplitude operators and impulse response functions. Results of a validation study are presented where model motion data in random waves was compared to predicted motion levels. The dependence of the craft's natural frequencies and damping characteristics on the overall dynamic performance of the craft in waves is discussed.

Introduction

As part of the Amphibious Assault Landing Craft (AALC) Program Office's technology development effort, the David W. Taylor Naval Ship Research and Development Center (DTNSRDC) has been constructing a Six Degree of Freedom (6DOF) motion simulations program for the two JEFF craft in waves. The simulations are based on empirical data: i.e., the model data taken in the towing tank and wind tunnel. The calm water maneuvering and control program for both craft was completed in 1974.[1,2] The purpose of this paper is to describe the method used to predict the pitch and heave motion in waves, and to present and discuss the on-cushion dynamic performance characteristics of the craft while operating in head waves.

Description of Craft and Model

The AALC is an air cushion vehicle (ACV) designed primarily to transport war material from off-shore stationed ships to a beach or staging area in unfavorable environmental conditions at high speeds.

Principal characteristics of the two prototype craft are given in Ref. 3. The skirt system of the JEFF (B) craft is of the bag and finger type and the air cushion is subdivided into four compartments. The JEFF (A) craft has a peripheral cell skirt/stabilization system and an undivided air cushion. Photographs of models of both craft are shown in Fig. 1.

The models used to obtain data on the dynamics of both craft were equipped with lift fans, ducting, and a flexible skirt system so that on-cushion overwater performance was simulated in model towing tank experiments.

Experimental Data Used in the Analysis

This is a linearized analysis of the pitch-heave response of the JEFF craft in head seas and is based upon experimental data obtained in earlier investigations. The coefficients (i.e. stability derivatives) in the equations of motion were obtained from oscillation experiments in pitch and heave. These experiments consisted of towing the models at various speeds while operating on-cushion at the scaled design cushion pressure. The models were then oscillated in both pitch and heave (separately) over a range of frequencies from 1/4, to 2 Hz. Amplitudes of oscillation of 1/4, 1/2, and one inch (6.35, 12.7 and 25.4 mm) were used. The resulting forces and moments on the models were measured using block gage assemblies. The fundamental harmonics of the unsteady forces and moments were resolved into components in-phase and out-of-phase with the oscillatory motion. The force data was reduced by subtracting inertial and friction tares and the resulting coefficients were nondimensionalized using conventional stability and control techniques.[4]

The oscillation experiments were conducted at Froude-scaled model speeds corresponding to 35 and 50 knots full scale. The nondimensional derivatives were found to be highly dependent upon Froude number. Since the motion prediction was to be correlated to motion data at 30 and 40 knots, it was necessary to linearly interpolate and extrapolate the derivatives to these speeds. The resulting nondimensional stability derivatives are listed in Table 1.

Another series of experiments was conducted to obtain the wave excitation forces and moments. These experiments used essentially the same test setup as the oscillation experiments. The craft height was held fixed at the design equilibrium height, and with attitude and cushion pressure held constant, the model was run through regular head waves produced by a pneumatic wavemaker located at the end of the towing basin. The resulting heaving forces and pitching moments were obtained at 35 and 50 knots (full scale) for various wavelengths.

Frequency and Time Domain Results

The model data described in the preceding section has been applied to a linearlized pitch-heave analysis of the craft. Typical numerical results are given in this section, along with a condensed description of the analysis.

Table 1 JEFF (B) nondimensional stability derivatives

Derivative	30 knots ($F_n = 1.$)	40 knots ($F_n = 1.33$)
Z'_h	−0.687	−0.625
$Z'_{\dot{w}}$	0.0017	−0.0009
Z'_w	−0.2104	−0.2077
Z'_θ	0.1326	0.1199
Z'_q	−0.0049	0.0030
$Z'_{\dot{q}}$	−0.0005	−0.0005
M'_h	0.0613	0.04
$M'_{\dot{w}}$	0.0059	0.0037
M'_w	−0.0151	−0.0110
M'_θ	−0.0379	−0.0237
$M'_{\dot{q}}$	−0.0004	−0.0004
M'_q	−0.0086	−0.00668

Presented as Paper 76-865 at the AIAA/SNAME Advanced Marine Vehicles Conference. Arlington, Va., Sept. 20-22, 1976; submitted Sept. 20, 1976; revision received Feb. 9, 1977.

Index categories: Marine Vessel Trajectories, Stability, and Control.

*Naval Architect.

†Mathematician.

Frequency Response Matrix

The equations of motion in pitch and heave in the frequency domain may be written as follows

$$\begin{aligned} a_{33}(\omega)\ h_0(\omega) + a_{35}(\omega)\theta_0(\omega) &= -Z_0 \\ a_{53}(\omega)\ h_0(\omega) + a_{55}(\omega)\theta_0(\omega) &= -M_0 \end{aligned} \tag{1}$$

where h_0, θ_0, Z_0 and M_0 are the complex heave, pitch, normal force and pitching moment, respectively. The sign conventions and notations are illustrated in Fig. 2. Each of the four $a_{ij}(\omega)$ factors is a complex function given as follows

$$\begin{aligned} a_{33}(\omega) &= -[C_{33} - \omega^2(m + A_{33}) + i\omega B_{33}] \\ a_{35}(\omega) &= -[C_{35} - \omega^2 A_{35} + i\omega B_{35}] \\ a_{53}(\omega) &= -[C_{53} - \omega^2 A_{53} + i\omega B_{53}] \\ a_{55}(\omega) &= -[C_{55} - \omega^2(I_y + A_{55}) + i\omega B_{55}] \end{aligned} \tag{2}$$

The A_{ij}, B_{ij} and C_{ij} factors are related to the stability derivatives[4] as follows

$$\begin{aligned} A_{33} &= -Z_{\dot{w}} & A_{53} &= -(M_{\dot{w}} + mx_G) \\ B_{33} &= -Z_w & B_{53} &= -M_w \\ C_{33} &= -Z_h & C_{53} &= -M_h \\ A_{35} &= -(Z_{\dot{q}} + mx_G) & A_{55} &= -M_{\dot{q}} \\ B_{35} &= -(Z_q + Z_{\dot{w}}U) & B_{55} &= -(M_q + M_{\dot{w}}U) \\ C_{35} &= -(Z_\theta + Z_w U) & C_{55} &= -(M_\theta + M_w U) \end{aligned} \tag{3}$$

where x_G is the distance of the center of gravity from the reference point (the design center of gravity), and U is the craft speed. Nondimensional values for the stability derivatives listed in Eq. (3) are presented in Table 1 for the JEFF (B) craft at two speeds.

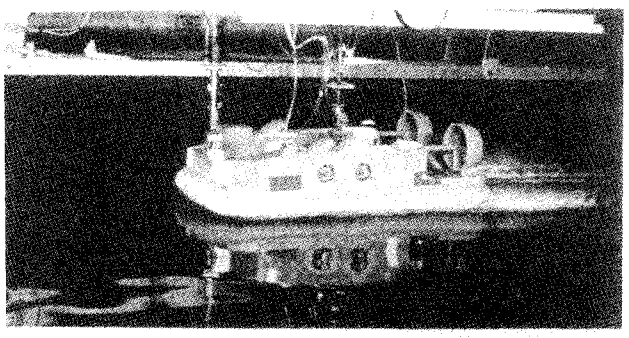

a) JEFF (B) model

b) JEFF (A) model

Fig. 1 JEFF craft models.

We may readily solve Eq. (1) for the pitch and heave, giving the following result in matrix form

$$\begin{bmatrix} h_0(\omega) \\ \theta_0(\omega) \end{bmatrix} = \begin{bmatrix} H_{33}(\omega) & H_{35}(\omega) \\ H_{53}(\omega) & H_{55}(\omega) \end{bmatrix} \begin{bmatrix} Z_0 \\ M_0 \end{bmatrix} \tag{4}$$

The 2×2 matrix in Eq. (4) is the frequency response matrix in pitch and heave. Each element $H_{ij}(\omega)$ of the matrix represents the complex motion response in the ith degree of freedom (mode) to a unit sinusoidal force excitation in the jth degree of freedom. The amplitude and phase angle of each of the elements of the frequency response matrix were calculated for both craft. A typical frequency response function for the JEFF (B) craft is presented in normalized form in Fig. 3 for a full scale speed of 40 knots at the design operating condition ($x_G = 0$). The H_{33} function in Fig. 3 has been normalized by dividing by its zero frequency limit. One can see from the figure that the force response is underdamped with a natural frequency of about 3 radians per second, or one half Hertz.

Impulse Response

The frequency domain characterization given by the frequency response matrix has associated with it a parallel time-domain characterization. The time domain charac-

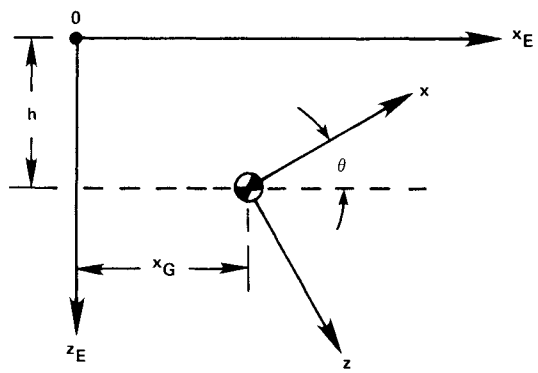

Fig. 2 Coordinate system used for pitch-heave analysis.

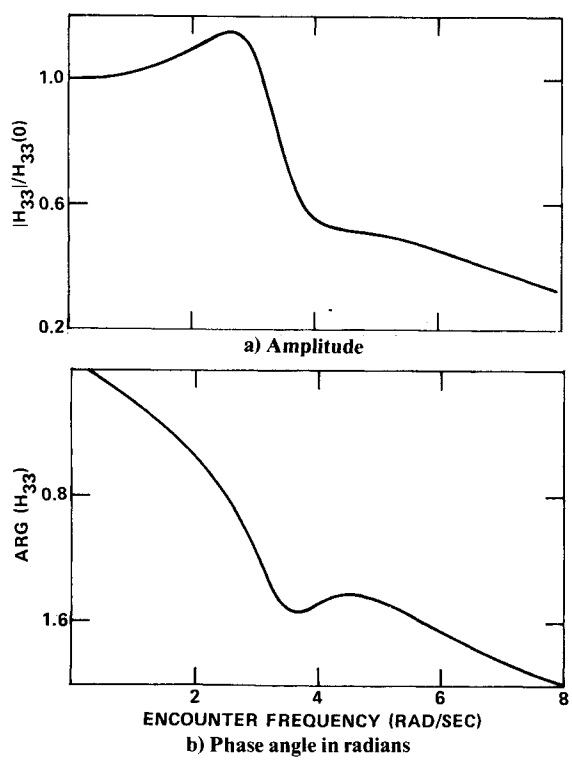

Fig. 3 Normalized heave frequency response for unit heave force (H_{33}), $V_K = 40$, Froude number = 1.33.

terization is given in terms of an array of impulse response functions. The time domain parallel to Eq. (4) is the following

$$h(t) = \int_{-\infty}^{\infty} h_{33}(\tau)\ Z_{ext}(t-\tau)\,d\tau + \int_{-\infty}^{\infty} h_{35}(\tau)\ M_{ext}(t-\tau)\,d\tau \tag{5}$$

$$\theta(t) = \int_{-\infty}^{\infty} h_{53}(\tau)\ Z_{ext}(t-\tau)\,d\tau + \int_{-\infty}^{\infty} h_{55}(\tau)\ M_{ext}(t-\tau)\,d\tau \tag{6}$$

where the $h_{ij}(t)$, $i,j=3$ or 5 represent responses in ith mode to unit impulsive forces in the jth mode and Z_{ext} and M_{ext} are externally applied excitation forces. Each of the elements of the impulse response matrix ($h_{ij}(t)$, $i, j=3$ or 5) is the Fourier integral transform of the corresponding frequency response function $H_{ij}(\omega)$, e.g.

$$h_{33}(t) = \frac{1}{2\pi}\int_{-\infty}^{\infty} H_{33}(\omega)e^{i\omega t}d\omega \tag{7}$$

Each of the force impulse response functions must be causal; i.e.

$$h_{ij}(t) = 0, \quad t<0, \quad i,j=3 \text{ or } 5$$

Examples of normalized impulse response functions are shown in Figs. 4 and 5 for JEFF (B) craft at 40 knots. These functions were normalized by dividing by the zero frequency limit of the respective frequency response function. The period of oscillation (2 sec) is consistent with the natural frequency found in the frequency response functions.

Frequency Response in Waves

To obtain the pitch and heave motion in regular waves as a function of the encounter frequency, use is made of Eq. (4) where the expressions for the wave excitation heave force and pitching moment are substituted for the externally applied harmonic force Z_0 and moment M_0. The motions are characterized by frequency response functions; i.e., heave and pitch motion per unit wave amplitude. The heave frequency response function from Eq. (4) is

$$(h_0/\eta_0) = (Z/\eta_0)_w\ H_{33}(\omega_e) + (M/\eta_0)_w\ H_{35}(\omega_e) \tag{8}$$

Similarly, the pitch angle frequency response per unit wave amplitude is given as

$$(\theta_0/\eta_0) = (M/\eta_0)_w H_{55}(\omega_e) + (Z/\eta_0)_w H_{53}(\omega_e) \tag{9}$$

Alternatively, the pitch angle frequency response may be expressed on a per unit wave slope basis, or

$$(\theta_0/\theta_{w0}) = (\lambda/2\pi)\cdot(\theta_0/\eta_0) \tag{10}$$

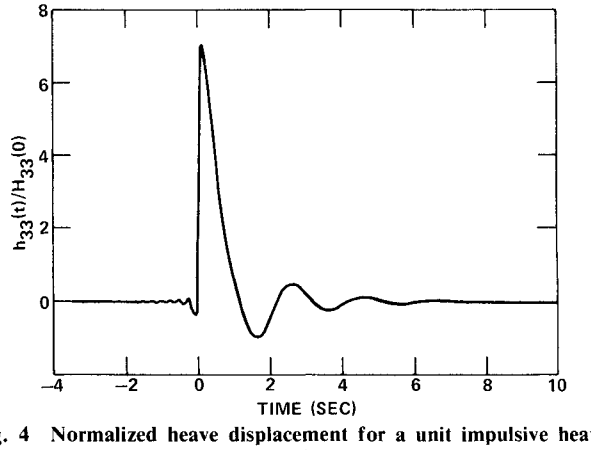

Fig. 4 Normalized heave displacement for a unit impulsive heave force, $V_K = 40$, Froude number = 1.33.

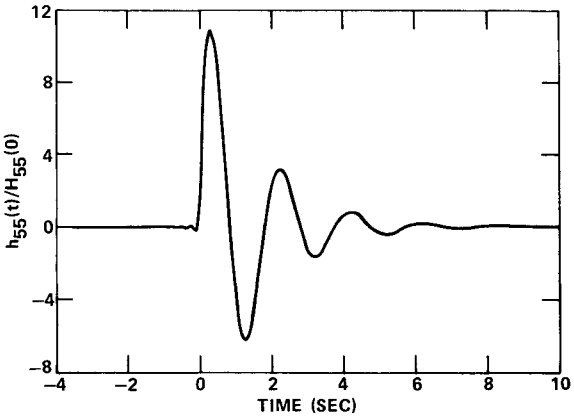

Fig. 5 Normalized pitch angle for a unit impulsive pitching moment, $V_K = 40$, Froude number = 1.33.

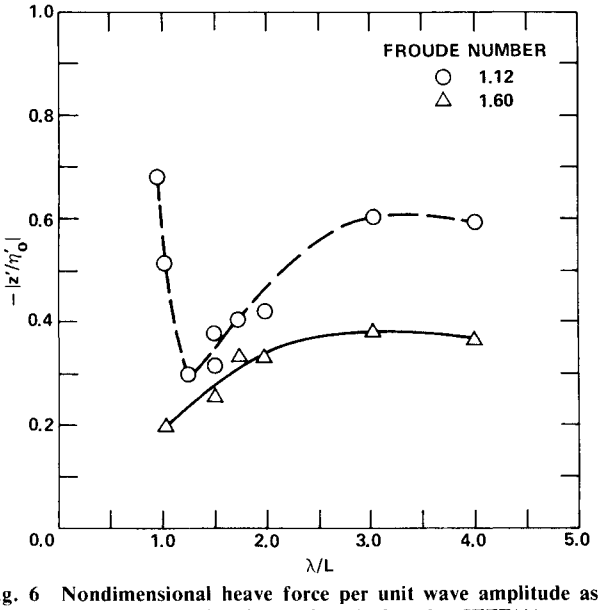

Fig. 6 Nondimensional heave force per unit wave amplitude as a function of nondimensional wavelength for the JEFF(A) at two speeds.

The heave force per unit wave amplitude in Eqs. (8 and 9) may be expressed as

$$(Z/\eta_0)_w = |Z'/\eta_0'|e^{i\phi_z}[(\rho U^2\ell)/2] \tag{11}$$

Similarly, the pitching moment per unit wave amplitude may be written

$$(M/\eta_0)_w = |M'/\eta_0'|e^{i\phi_m}[(\rho U^2\ell^2)/2] \tag{12}$$

The nondimensional form of the heave force per unit wave amplitude and its phase angle are given as a function of wavelength per unit cushion length (λ/L) for two speeds for the JEFF (A) model in Figs. 6 and 7.

The frequency response function for bow motion is related to the heave and pitch frequency response functions as follows

$$(-h_B/\eta_0) = -(h_0/\eta_0) + x_B(\theta_0/\eta_0) \tag{13}$$

where x_B is the distance from the reference point (the design LCG) to the bow. Heave and bow motion frequency response functions are shown for the JEFF (B) at 40 knots in Figs. 8 and 9. The responses are seen to be underdamped with a natural frequency of about 3 radians per second.

Experimental values for the maximum magnification factors at resonance in pitch and heave at 30 and 40 knots

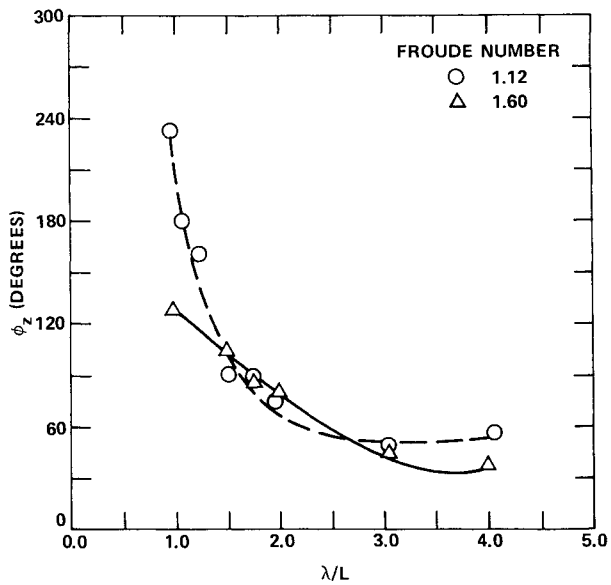

Fig. 7 Phase angle in degrees for heave force as a function of nondimensional wavelength.

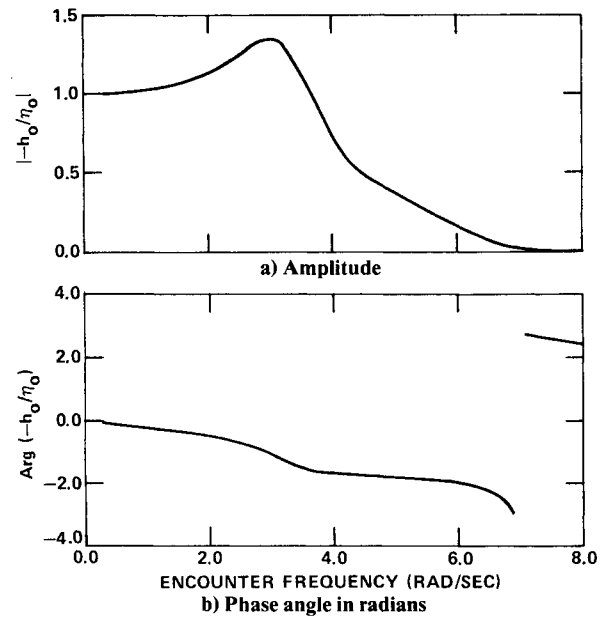

Fig. 8 Heave frequency response function in head waves, $V_K = 40$, Froude number = 1.33.

were obtained from an earlier motions experiment in random head waves. These data points are shown in Fig. 10. The curves indicate the values obtained from the simulation. Linear extrapolation was used in the 40 to 50 knots speed range. It is apparent from the motions data that for this particular configuration, the effective damping in pitch and heave decreases with speed resulting in more oscillatory behavior as speed increases.

Correlation with Random Wave Data

Model experiments on the C150-50 models of the JEFF (A) and (B) craft were performed in random head waves in the DTNSRDC Deep Water Basin in 1970. The data was presented in terms of power spectral density plots, response amplitude operators, nondimensional transfer functions, and double amplitude distribution functions. Data was presented for waveheight, pitch angle, roll angle, heave motion, and bow acceleration.

Since no regular wave data was taken, it was not possible to obtain a direct comparison between predicted frequency response functions like those shown in Figs. 8 and 9 and the motion data. To compare predicted responses to the experimental responses, response amplitude operators (RAOs) were derived from the frequency response functions. Then the input, the experimental waveheight spectrum, was used together with the predicted RAOs to obtain craft response spectra that could be compared directly to the experimental motion and acceleration specta.

The RAOs for heave, pitch, and bow acceleration are simply the squares of the amplitudes of the respective frequency response functions. The response spectra are computed by multiplying the appropriate RAO times the wave spectrum. For example, the heave spectrum (S_z) in $m^2 \cdot s$ is given as

$$S_z(\omega_e) = S_w(\omega_e)\ \mathrm{RAO}_z(\omega_e) \tag{14}$$

where $S_w(\omega_e)$ is the waveheight spectrum in $m^2 \cdot s$ as a function of the encounter frequency.

The variance (σ^2) was obtained by taking the area under the spectra: e.g.

$$\sigma_z^2 = \int_0^\infty S_z(\omega_e)\, d\omega_e \tag{15}$$

For a narrow band signal the significant level (average highest 1/3 double amplitude) is four times the standard deviation (σ) or, for example

$$\text{Significant Heave} = 4\sigma_z \tag{16}$$

The results of the correlation for the JEFF (B) are shown in Figs. 11 through 13 for a run in a Sea State 2 at 40 knots. Figure 11 shows the waveheight spectrum as a function of the encounter frequency. The pitch angle spectrum is shown in Fig. 12. The large scale plot is the predicted spectrum and the small insert is the experimental spectrum.

The predicted and measured bow acceleration spectra are shown in Fig. 13. Note that the shape of the spectra correlate

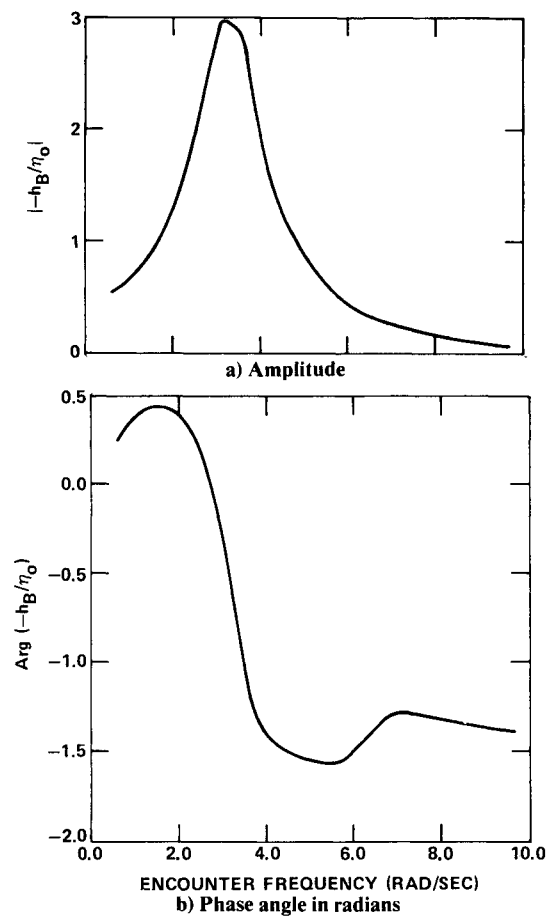

Fig. 9 Frequency response function for bow motion in head waves. $V_K = 40$, Froude number = 1.33.

well in the sense that the energy content of the response lies in the correct frequency range; however there is some discrepancy in the fine detail of the spectra.

A quantitative measure of the correlation between predicted and measured responses is given in terms of significant response levels in Table 2. The significant levels for the run shown in Figs. 11 through 13 are shown on line 4 of the Table. The correlation is very close for heave, pitch angle, and bow acceleration. Four other random wave runs were compared to predictions in the same manner as shown in lines 1, 2, 3 and 5 of Table 2. Line 1 is a 30 knot Sea State 2 run with LCG shifted forward 5% of the craft length. The LCG shift was taken into account in the predictions. The pitch angle was overpredicted by about 12%, but the heave and bow acceleration correlation was very good. Line two shows the results for a 30 knot run in a Sea State 3. The significant heave and bow acceleration predictions are very close. The pitch is overpredicted by about 10%.

Line 3 shows results for a speed of 30 knots, in a Sea State 4 at the design LCG and weight. Finally, line 5 is for a speed of 40 knots in a Sea State 2 in an overweight condition. Again the appropriate physical parameters were introduced in the predictions of the overweight run.

For all five runs the same quantitative trends hold: i.e., the heave and bow acceleration predictions are very close while the pitch angles are overpredicted by up to 14 percent at 30 knots. The pitch angle correlation is much better at 40 knots than at 30 knots.

Time-Domain Response to Regular Waves

The craft response has been calculated in the time-domain for regular waves having several different wavelengths. The results are presented here to demonstrate the correspondence between the time and frequency domain approaches. These calculations were carried out to verify the feasibility of calculating time domain responses from the impulse response matrix using numerical techniques. The response was computed using the convolution integral representation given in Eqs. (5 and 6). The external heave force and pitching moment due to waves were substituted into the integrals. If the wave elevation at the LCG is taken as

$$\eta(t) = \eta_0 \sin\omega_e t \tag{17}$$

the wave force and moment can be written, using Eq. (11 and 12).

$$Z_{\text{wave}}(t) = (Z/\eta_0)_w \eta_0 \sin(\omega_e t + \phi_z)$$
$$M_{\text{wave}}(t) = (M/\eta_0)_w \eta_0 \sin(\omega_e t + \phi_M) \tag{18}$$

In addition, the absolute bow motion is given as follows

$$h_B = h(t) - x_B\theta(t) \tag{19}$$

and the wave elevation at the bow is

$$\eta_B = \eta_0 \sin(\omega_e t + (2\pi/\lambda)x_B) \tag{20}$$

Figures 14 and 15 show the wave elevation, heave and bow motion for $\lambda/L = 2.02$, $\omega_e = 3.75$ (rad/sec) and a waveheight of 2.3 ft (0.70m). This frequency is slightly above the resonant, and one can see a slight attenuation of heave in Fig. 14.

The mean heave and bow motion have been shifted five feet (1.524m – the cushion height) above the wave troughs so that wave contact with the hard structure could be observed directly. The shift was made relative to the wave troughs

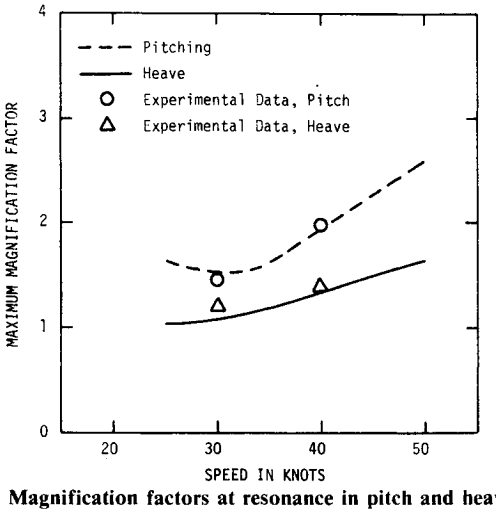

Fig. 10 Magnification factors at resonance in pitch and heave as a function of craft speed for the JEFF (B).

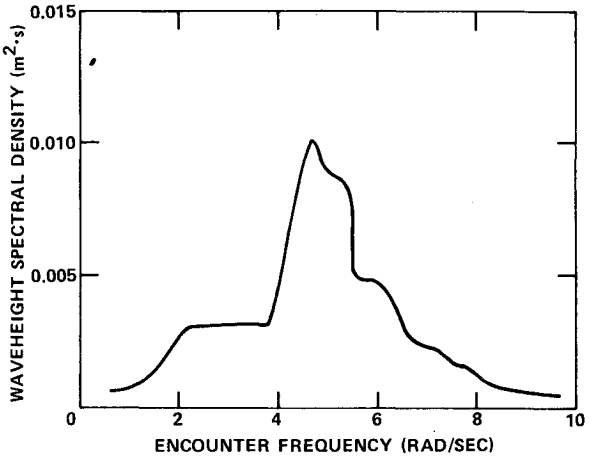

Fig. 11 Power spectral density of encountered waveheight, $V_K = 40$, significant waveheight = 2.2 ft (0.67 m).

Table 2 Comparison of predicted and measured significant responses for JEFF (B) for various speeds and sea states

			Sig. Heave (m)		Pitch angle (deg)		Sig. bow accel (g's)	
V_K	Sea state	Sig W.H.(m)	Meas.	Pred.	Meas.	Pred.	Meas.	Pred.
30	2 5%LCG	0.75	0.46	0.46	2.88	3.28	0.96	1.02
	3	1.01	0.74	0.74	5.43	6.05	1.71	1.65
	4	1.98	1.77	1.69	10.3	11.73	2.74	2.85
40	2	0.67	0.45	0.45	3.39	3.44	1.42	1.44
	2 1.25%P.L.	0.67	0.48	0.50	3.86	3.58	1.45	1.36

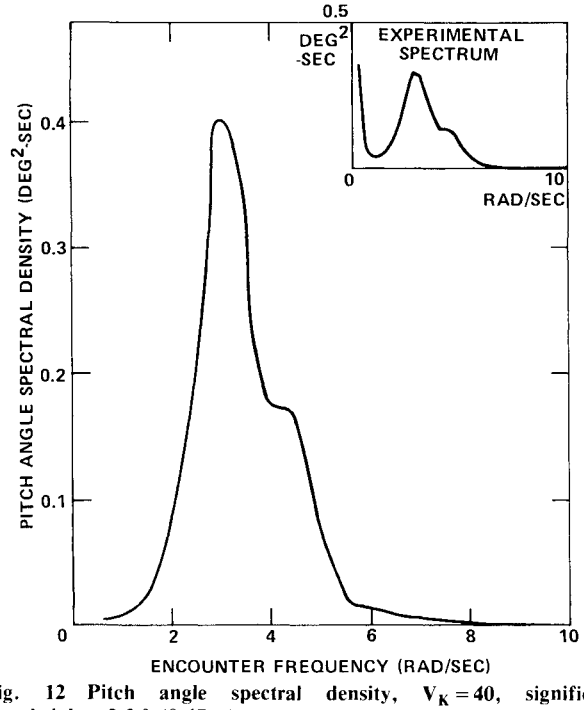

Fig. 12 Pitch angle spectral density, $V_K = 40$, significant waveheight = 2.2 ft (0.67 m).

because it was assumed that the craft settles to this mean flying height so that the skirt leakage area remains approximately the same in calm and rough water. This drop in mean flying height in waves has been observed in model experiments.[5]

Figure 15 shows the wave elevation at the bow computed from Eq. (20), and the shifted bow motion, computed from Eq. (19) for the same conditions as Fig. 14. This plot shows how the forward extremity of the underside of the craft hard structure is moving relative to the wave elevation at the same point. One sees from the figure that the two curves approach each other closely, implying that a slight increase in waveheight will produce water contact at the bow and possibly wave impact.

Computer runs similar to Figs. 14 and 15 were made for other wavelengths, i.e. other encounter frequencies. At the lower frequencies (longer wavelengths) the craft tends to contour or follow the wave, so that the craft can negotiate considerably larger waves without impact occuring. At the high frequencies (short wavelengths) the absolute motions

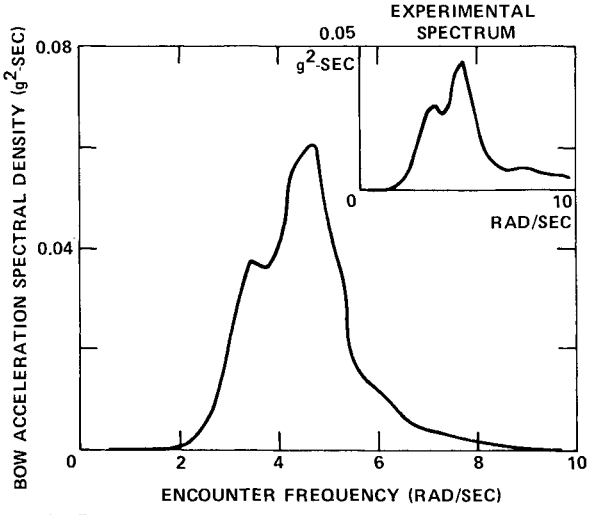

Fig. 13 Bow acceleration spectral density, $V_K = 40$, Significant waveheight = 2.2 ft (0.67m).

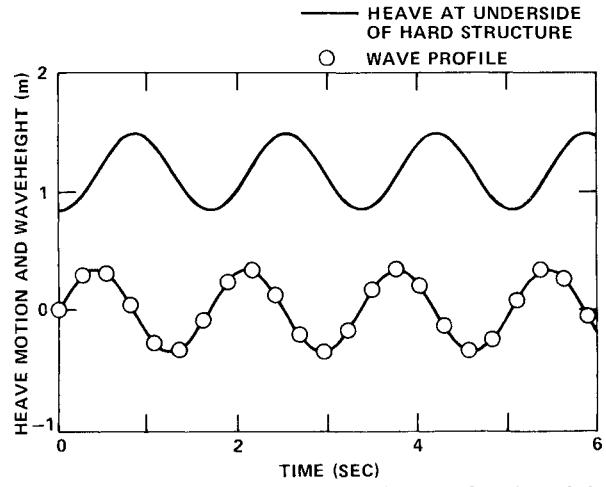

Fig. 14 Heave response and wave elevation as a function of time, $V_K = 40$, $\lambda/L = 2.02$, encounter frequency = 3.75 rad/sec, waveheight = 2.3 ft (0.70 m).

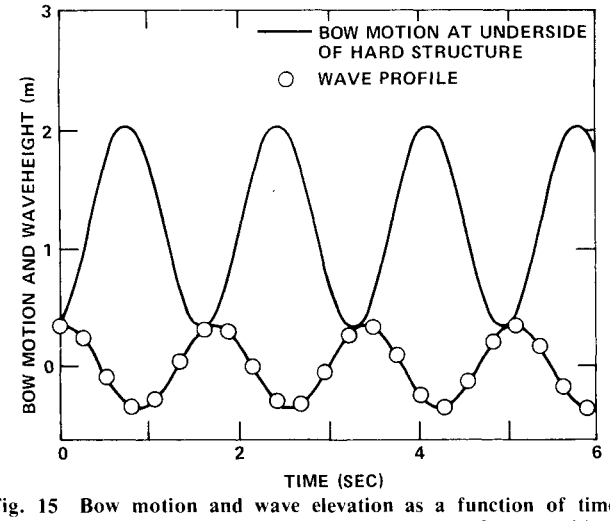

Fig. 15 Bow motion and wave elevation as a function of time, $V_K = 40$, $\lambda/L = 2.02$, encounter frequency = 3.75 rad/sec, waveheight = 2.3 ft (0.70 m).

become small so that the craft can negotiate waves with heights approaching the cushion depth without bow impact.

Summary and Discussion

The pitch and heave dynamics of the JEFF craft have been analyzed in the time and frequency domain. The linearized analysis is based on experimental data obtained from pitch and heave oscillation and captive-model wave excitation experiments. Typical force response characteristics at 40 knots in the time and frequency domain are plotted in Figs. 3, 4, and 5.

The craft response in waves is characterized by frequency response functions. Heave per unit waveheight and bow motion per waveheight are shown in Figs. 8 and 9. For the JEFF (B) craft the heave and bow motion response is seen to be underdamped, with a natural frequency of about 3 radians per second or 1/2 Hz. This natural frequency is also evident in the force frequency response function (Fig. 3) and the impulse response functions (Figs. 4 and 5). The magnification at resonance for the bow motion is higher than heave because of the pitching contribution. The underdamped behavior in pitch is also evident from Fig. 5.

The magnification factors at resonance in pitch and heave taken from the wave frequency response functions, are shown as a function of craft speed in Fig. 10. One can see clearly that the effective damping in both heave and pitch decreases with

increasing speed; i.e. the craft response tends to become more oscillatory as the speed increases. The pitch motion has less damping than the heave motion for the whole speed range. The natural frequency remained constant (at about 3 radians per second) at speeds from 25 to 50 knots. The predicted JEFF (B) frequency response in waves can be compared with full-scale trial results of the British BH.7 hovercraft using data reported in Refs. 1 and 6. Pitch and heave response amplitude operators for the BH.7 were obtained in head seas in a Sea State 2. The craft speed corresponded to a Froude number of about 1.7 for the 50 ton (110,000 pound) craft. The resonant frequency was about 2.2 radians per second for both pitch and heave. The peak magnification was 1.2 for heave and 1.3 for pitch. The natural frequency and peak magnifications were lower than observed for the JEFF (B). That is, the BH.7 appears to have more damping even though the Froude number was higher. The quantitative difference in response may be partly caused by weight differences: the JEFF (B) weighs about 3 times the BH.7, even though they are about the same size and have the same type of cushion and skirt system. Another possibility is that scale effects may be present. Still another possibility is that the wave spectrum in the trials may have been distributed over a range of directions. At any rate, the qualitative behavior of the pitch and heave dynamics for both craft appears to be the same: both are underdamped and the pitch is more so than the heave. In addition, the natural frequencies are fairly close.

Results of the correlation with the random wave motions data are shown in Figs. 11 through 13 for a 40 knot run in a Sea State 2. The figures show the power spectral density for the waveheight, pitch angle, and bow acceleration. The motion and acceleration predictions used the experimental wave height as the input and appropriate response amplitude operators predicted from the linear analysis. One can see that the spectral energy distribution agrees well qualitatively.

A quantitative evaluation of the correlation is shown in Table 2 for five runs. The correlation is based on significant (average 1/3 highest double amplitude) values derived from the area under the spectra. The correlation in heave and bow acceleration is very close, within about 5% at 30 knots. Better correlation in pitch occurs at 40 knots. The overprediction in pitch is caused by the shape of the predicted pitch response spectra, which are more sharply peaked and somewhat narrower than the experimental spectra. The good correlation with bow acceleration indicates that the phase angle relationship between heave and pitch must be realistic because bow acceleration is derived from both types of motion.

Time domain response in regular waves at 40 knots is shown in Figs. 14 and 15. The responses were obtained from the impulse response matrix using convolution integrals.

At 40 knots the craft can negotiate waves of any length without wave contact at the bow provided that the waveheight does not exceed 2.3 ft. (0.7m – just over 1/2 the nominal cushion height). The worst case occurs at an encounter frequency just above the natural frequency where the wavelength is about twice the cushion length. At lower frequencies the craft tends to follow or contour the waves and at higher frequencies the motion becomes increasingly attenuated so that waves with heights approaching the cushion depth can be negotiated.

Similar bow motion behavior was observed on the XR-5 High L/B model where relative bow motion was measured using an ultrasonic probe.[7] The worst case occurred at a frequency slightly higher than the natural frequency and at a wavelength of about twice the cushion length. Wave contact at the bow occurred for a waveheight of 1/3 the cushion depth.

The importance of relative bow motion cannot be overemphasized. The relative bow motion provides a direct quantitative measurement of bow slamming or wave impact. The occurrence of severe wave impacts may jeopardize the craft's survivability at high speeds. More experimental work is required to develop quantitative criteria relating frequency and severity of bow impacts to relative bow motion.

Figure 29 of Ref. 8 shows speed reduction in waves as a function of sea roughness parameter. It appears that the reduction in speed for air cushion craft is more abrupt than for hydrofoils. One may expect the speed reduction to be caused by propulsive power limitations, slamming and wave impacts (safety), or ride comfort, or combinations of these.

The characteristic rapid dropoff in speed with sea state experienced by air cushion supported craft drastically reduces their effectiveness for commerical and military applications. Any improvement of the design of these craft that extends the operational envelope would be very effective in increasing the craft's utility.

One major cause of speed dropoff with sea state is the nature of the dynamic response in waves. It has been shown that wave impacts will occur at the bow for relatively small waveheights at the resonant encounter frequency. This underdamped response is highly undesirable, particularly for craft designed for high speed operation.

This type of bow motion response is typical of air cushion supported vehicles, and is caused by a combination of inadequate pitch-heave damping and the phase relationship between pitch and heave. Figure 5 shows the underdamped pitch angle response which is characteristic of these craft.

The net effect of the underdamped response is to decrease the effectiveness of the air cushion and skirt system in elevating the craft hard structure above the waves. That is, for certain frequencies the craft cannot negotiate waves equal to the cushion depth, so some of the air cushion depth is wasted. Hydrofoil craft, on the other hand, can negotiate waves up to the strut length, regardless of the wave frequency because the craft is optimized by suitable adjustment of feedback gains in the hydrofoil control system. This is probably a major cause of the difference in speed loss with sea state for the two craft types.

To improve the response characteristics of the craft one can provide for automatic regulation of the cushion and seal pressures. Active pitch and roll motion compensation can be achieved on the BHC-type subdivided air cushion by regulation of the air feed to the various cushion compartments. Motion compensation of the peripheral cell stabilized craft can be achieved by automatic control of the pressures of groups of cells arranged in quadrants.

Although this paper is based entirely upon linear theory, it is well known that the air cushion dynamics involve nonlinear effects. Nevertheless, for motion and acceleration prediction of these craft, nonlinearity does not appear to be a serious problem. The correlation of motion data to predictions based on linear theory did not deteriorate when the sea state was increased from 2 to 4 (see Table 2). This result implies that there is little amplitude dependence in the response, contrary to what would be expected if nonlinear effects were important.

A partial linearity investigation on the XR-5 response in regular and random waves was reported in Refs. 5 and 9. It was found that heave motion, pitch angle, relative bow motion, and bow acceleration all exhibited reasonably linear behavior for the wave heights investigated. Some nonlinear response was observed for heave acceleration, although it was not considered serious enough to justify abandoning linear theory for motion prediction. The results of the present investigation tend to confirm this conclusion.

The entire analysis has assumed that the model scale coefficients in the equations of motion can be extrapolated to full scale using Froude scaling. However, it is well known that the dynamics of the air cushion and skirt system are not governed solely by Froude scaling. The motions (pitch and heave) are probably less affected by the scaling errors than heave acceleration. Note that the pitch and heave RAOs of the BH.7 were similar to the predicted JEFF (B) RAOs.

Acknowledgments

The authors wish to acknowledge the overall guidance and encouragement of M. D. Ochi, Head, High Performance Craft Dynamics Branch. J. A. Fein obtained the hydrodynamic coefficients in an earlier investigation and J. Kallio conducted the random wave motion experimental program. The support, guidance and encouragement of Z. G. Wachnik of the Amphibious Assault Landing Craft Project Office is also gratefully acknowledged.

References

[1]Fein, J.A., Magnuson, A.H., and Moran, D.D., "Dynamic Performance Characteristics of an Air Cushion Vehicle," *Journal of Hydronautics,* Vol. 9, Jan. 1975, pp. 13-24.

[2]Wachnik, Z.G., Messalle, R.F., and Fein, J.A., "Control Simulation of Air Cushion Vehicles," *Proceedings of the Fourth Ship Control Systems Symposium,* The Hague, Netherlands, Oct. 1975.

[3]Brown, M.W., "Jeff Craft-Navy Landing Craft for Tomorrow," Presented at AIAA/SNAME Advanced Marine Vehicles Conference, AIAA Paper No. 74-319, San Diego, Calif., Feb. 1974.

[4]Gertler, M. and Hagen, G.R., "Standard Equations of Motion for Submarine Simulation," NSRDC Report 2510, June 1967.

[5]Ricci, J.J. and Magnuson, A.H., "Seakeeping Characteristics of the XR-5, A High Length-to-Beam Ratio Manned Surface Effect Testcraft: III Results of Random Wave Experiments, Investigation of Linear Superposition for Ship Motions and Trim and Draft in Random Waves," DTNSRDC Report SPD 616-03, May 1976.

[6]Magnuson, A.H., "Seakeeping Trials of the BH.7 Hovercraft," NSRDC Ship Performance Department Report SPD-574-01, Aug., 1975.

[7]Magnuson, A.H. and Wolff, K.K., "Seakeeping Characteristics of the XR-5, A High Length-Beam Ratio Manned Surface Effect Testcraft: 1. XR-5 Model Response in Regular Head Waves," NSRDC Ship Performance Department Report SPD 616-01, March 1975.

[8]Mantle, P.J., "Cushions and Foils," Paper Presented at the Society of Naval Architects and Marine Engineers Spring Meeting, Philadelphia, Pa., June 1976 (To Appear in SNAME Transactions, 1976).

[9]Magnuson, A.H. and Wolff, K.K., "Seakeeping Characteristics of the XR-5, A High Length-to-Beam Ratio Manned Surface Effect Testcraft II. Results of Linearity Investigation, Effects of Changes from Reference Operating Condition and Trim and Draft in Regular Waves," NSRDC Ship Performance Department Report SPD-616-02, March 1975.